



Enantioselective transesterification catalysis by nanosized serine protease subtilisin Carlsberg particles in tetrahydrofuran

Betzaida Castillo^a, Yamixa Delgado^a, Gabriel Barletta^b, Kai Griebenow^{a,*}

^a Department of Chemistry, University of Puerto Rico, Río Piedras Campus, PO Box 23346, San Juan, Puerto Rico 00931-3346

^b Department of Chemistry, University of Puerto Rico, College at Humacao, CUH Station, Humacao, Puerto Rico 00791

ARTICLE INFO

Article history:

Received 1 October 2009

Received in revised form 12 January 2010

Accepted 13 January 2010

Available online 25 January 2010

Keywords:

Enantioselective catalysis

Non-aqueous enzymology

Enzyme

Secondary alcohol

Serine protease

ABSTRACT

Enzyme catalysis in organic solvents is a powerful tool for stereo-selective synthesis but the enantioselectivity is still hard to predict. To overcome this obstacle, we employed a nanoparticulate formulation of subtilisin Carlsberg (SC) and designed a series of 14 structurally related racemic alcohols. They were employed in the model transesterification reaction with vinyl butyrate and the enantioselectivities were determined. In general, short alcohol side chains led to low enantioselectivities, while larger and bulky side chains caused better discrimination of the enantiomers by the enzyme. With several bulky substrates high enantioselectivities with $E > 100$ were obtained. Computational modeling highlighted that key to high enantioselectivity is the discrimination of the *R* and *S* substrates by the sole hydrophobic binding pocket based on their size and bulkiness. While bulky *S* enantiomer side chains could be accommodated within the binding pocket, bulky *R* enantiomer side chains could not. However, when also the *S* enantiomer side chain becomes too large and does not fit into the binding pocket anymore, enantioselectivity accordingly drops.

© 2010 Elsevier Ltd. All rights reserved.

1. Introduction

The production of single enantiomers of chiral intermediates has become increasingly important in the pharmaceutical industry.¹ During the last few years, the synthesis of bio-relevant compounds and their precursors using enzymes in aqueous and non-aqueous media has been on the rise.² One of the most promising properties of enzymes is that they can be extremely selective due to their three-dimensional substrate binding site and active site structure. This selectivity can be utilized to introduce chirality into organic molecules, resolve racemic mixtures, and functionalize molecules regioselectively.^{2b,3} The usefulness of enzymatic catalysis in organic solvents for producing chiral precursors of biologically relevant compounds, such as, anti-tubercular drugs,⁴ β -adrenergic blocking agents,⁵ anti epileptic agents,⁶ potential anti-neoplastic agents,⁷ and drugs for the treatment of typhoid fever and other infectious diseases,⁸ is well recognized. However, the reduced activity and the lack of predictability of the selectivity in organic solvents are still major drawbacks.⁹

One of the reasons for the lack of predictability of enantioselectivity might be the fact that the necessary enzyme dehydration step, frequently performed by lyophilization, causes structural

changes.¹⁰ Generally, when the lyophilized enzyme catalysts are suspended in an organic solvent, the enzyme is locked in a non-native conformation resulting in a less active biocatalyst^{10c} and likely a less selective one as well.

Consequently, the development of formulations to improve enzymes for use as catalysts in organic solvents has been attempted frequently.^{2a,10c,11} Cyclodextrins are one of the most successful groups of additives that activate enzymes in neat organic solvents.^{11g} Griebenow et al. reported that methyl- β -cyclodextrin (M β CD) dramatically activates the serine protease subtilisin Carlsberg in organic solvents.^{11a} The results suggest that M β CD activates this enzyme by two mechanisms: it acts as a molecular lubricant enhancing enzyme dynamics and it reduces protein structural perturbations during lyophilization.^{11a-c} M β CD also improved enantioselectivity in the model reaction of *sec*-phenethyl alcohol and vinyl butyrate.^{11a}

Enzyme enantioselectivity in organic solvents has been scrutinized many times in the literature, but fundamental problems and arguments still remain. For example, the relationship between enzyme flexibility (structural dynamics) and enantioselectivity is being debated.¹² Most models explaining differential enantioselectivity in various solvents are typically based on differential binding of *R*- and *S*-enantiomer substrates to the respective binding pockets.^{12,13} It is, however, remarkable how much higher the enantioselectivity of enzymes typically is under natural conditions.^{12a} One explanation for this is that structural and/or

* Corresponding author. Tel.: +787 764 0000x4781; fax: +787 756 7717.

E-mail address: kai.griebenow@gmail.com (K. Griebenow).

dynamical changes occurring upon removal of enzymes from aqueous buffer and introduction into an organic solvent cause diminished enantioselectivity. There is ample evidence that enzyme structural preservation during this process leads to improved enantioselectivity.^{11a–c,14} We therefore argue that employing a structurally improved formulation of an enzyme should result in better experimental data on enantioselectivity when employing various racemic substrates. Furthermore, it should be possible to explain these data using computational modeling since the active site structure should be more similar to the one obtained by X-ray crystallography. Lastly, to remove as much experimental uncertainty as possible from the data, such an approach should be performed in one solvent only using one carefully selected enzyme formulation.

In this study, we selected subtilisin Carlsberg (SC) co-lyophilized with M β CD as the model system based on our past experiences.^{11a–c} The particle size of the powder after suspension in organic solvents is 110 \pm 20 nm and consequently there are no diffusional limitations even at accelerated reaction conditions.¹⁵ A series of 14 racemic secondary alcohols was employed as substrates in the transesterification model reaction with vinyl butyrate to explore the relationship between substrate structure and enantiomeric excess in detail. Finally, computational modeling was carried out to explain the data obtained. As the result of the investigation, we are able to present a consistent model of the enantioselectivity of the protease in the organic solvent THF.

2. Results and discussion

Enzymes rarely have the combined properties necessary for industrial chemical production of chiral compounds, such as, high activity and selectivity toward non-natural substrates. They are usually 10² to 10⁶ times less active in organic solvents than in water⁹ and show drastically reduced enantioselectivity.^{12a} In this study, SC was lyophilized from an aqueous buffer (pH 7.8) with or without M β CD, which is a reported strategy designed to ameliorate lyophilization- and organic solvent-induced partial denaturation or structural changes.^{11a–c} The preparations were suspended in THF and the kinetics of the product formation in the transesterification between different *sec*-alcohols and vinyl butyrate was followed by gas chromatography (Fig. 1).

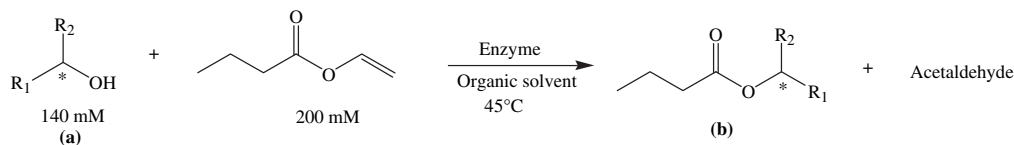


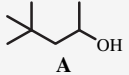
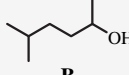
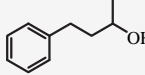
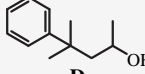
Figure 1. Transesterification reaction between vinyl butyrate and the racemic secondary alcohols catalyzed by subtilisin Carlsberg.

First, in order to establish feasibility of our approach using the M β CD containing subtilisin formulation, subtilisin prepared without and with M β CD was employed in four model reactions employing racemic secondary alcohols and initial rates and enantioselectivities were determined. In accordance with previous studies using other substrates,^{11a–c,f} our results show a 12- to 33-fold increase in the SC activity as the result of co-lyophilization with M β CD (see Table 1). In addition, enantioselectivity was improved using this preparation for all substrates initially tested.

We next proceeded to employ a series of 14 structurally different secondary alcohols in the model transesterification reaction using the SC-M β CD formulation solely (Table 2). To better understand the stereo and steric preferences of the enzyme, we employed four groups of secondary alcohols in which one parameter was changed systematically. The first group was chosen to systematically vary the length of the linear aliphatic chain of one of

Table 1

Initial rates and enantioselectivities for the product formation in the transesterification reaction of *sec*-alcohols with vinyl butyrate for different preparations of subtilisin C

Substrates	Enzyme preparation	$V_S^{a,b,c}$	Enantioselectivity ^d
 A	Lyophilized M β CD	1	93
		14	126
 B	Lyophilized M β CD	5	93
		59	141
 C	Lyophilized M β CD	7	82
		228	104
 D	Lyophilized M β CD	1	148
		32	240

^a Initial rates for the *S* enantiomer in nmol mg⁻¹ min⁻¹.

^b Enzyme concentration 1 mg/mL in all experiments.

^c Experiments were performed in duplicate. Results are the average of both trials.

^d Measured by the ratio of $[k_{cat}/K_M]_S/[k_{cat}/K_M]_R = V_S[R]/V_R[S]$.

the substituents at the stereocenter (substrates 1–5, Table 2). Interestingly, the enzyme enantioselectivity increased with increasing length of the linear carbon chain from 3 to 67 (Table 2).

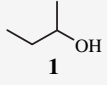
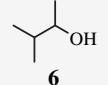
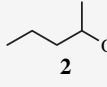
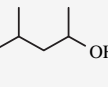
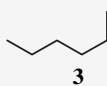
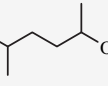
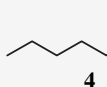
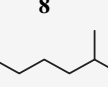
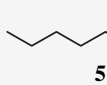
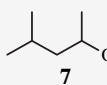
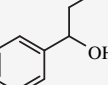
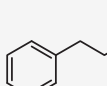
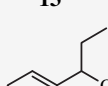
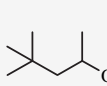
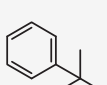
A linear correlation was observed between the enzyme enantioselectivity and the length of the linear aliphatic chain (Fig. 2). Each methylene group increased the enzyme enantioselectivity by about 17 units. The second group of secondary alcohols studied differs from the first one in that a methyl group was added and moved along the aliphatic chain from the beta to the epsilon carbons (substrates 6–9, Table 2). As with the previous group, we also observed in this case a linear increase in enantioselectivity with an increasing number of methylene groups in the aliphatic chain. However, maximum enantioselectivity is reached with 5-methyl-2-hexanol (substrate 8), decreasing sharply with the next substrate in which an additional methylene is added and the methyl group placed on the epsilon carbon (6-methyl-2-heptanol, substrate 9).

The enzyme enantioselectivity toward the first three alcohol substrates in this group increases about 65 units from one substrate to the next, more sharply than what was observed with the previous set of substrates discussed. This suggests that the added methyl group imposes steric constraints, which averts the *R* enantiomer from competing for the active site.

The third group of substrates was constructed by varying substituents at the gamma carbon (Table 2). In general, the enantioselectivity increased with increasing size and thus steric effect of the substituent at the gamma carbon. For example, adding an additional methyl group to the gamma carbon (as in 4,4-dimethyl-2-pentanol, substrate 11) increases the enzyme enantioselectivity substantially as compared to substrate 7 (4-methyl-2-pentanol). The alcohol substrate for which the enzyme was found to be most enantioselective was 4-methyl-4-phenyl-2-pentanol (substrate 12, *E*=240), in which the steric effect at the gamma carbon is increased

Table 2

Initial rates and enantioselectivities for the product formation in the transesterification reaction of different *sec*-alcohols with vinyl butyrate for subtilisin Carlsberg co-lyophilized with M β CD

Substrates	V_S^a	V_R^a	E^b	Substrates	V_S^a	V_R^a	E^b
First group				Second group			
	177	59	3		255	28	9
	246	12	20		139	1.9	73
	102	2.3	44		59	0.4	141
	99	1.7	58		209	2.6	80
	183	2.7	67				
Third group				Fourth group			
	139	1.9	73		74	1.4	51
	228	2.2	104		49	24.5	2
	14	0.1	126 ^c				
	32	0.1	240 ^c				

^a Initial rates for the *S*- and *R*-enantiomer in nmol mg⁻¹ min⁻¹.

^b Measured by the ratio of $[k_{cat}/K_M]_S/[k_{cat}/K_M]_R = V_S[R]/V_R[S]$.

^c Enantioselectivity could not be determined accurately because of the very low value of V_R .

by the aromatic group. The latter is a derivative of 2-pentanol, which is a key chiral intermediate required for synthesis of anti-Alzheimer drugs that inhibit β -amyloid peptide release and/or its synthesis.¹⁶

Two additional secondary alcohols were tested: 1-phenyl-1-propanol and 1-*p*-tolyl-1-propanol (substrates **13** and **14**), and the enzyme enantioselectivity was found to be lower than for most of the other substrates tested.

Finally, we investigated whether the enantioselectivity and activity changes were related. No correlation was evident when plotting the initial rate for the *S* enantiomer (V_S) versus enantioselectivity ($R < 0.5$, data not shown). These results contrast the data reported by Broos et al. where a correlation between enzyme enantioselectivity and initial rates was found.^{12c}

Our data show some remarkable trends. First, increasing the length of the linear aliphatic chain of one of the substituents at the

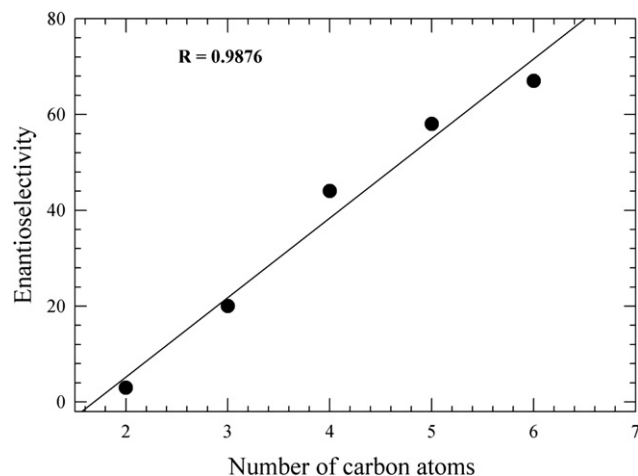


Figure 2. Effect of the length of the linear aliphatic chain of one of the substituents at the stereocenter of the substrates **1–5** on enzyme enantioselectivity.

stereocenter caused higher enantioselectivity (Fig. 2). Second, adding more bulky substituents increased the enantioselectivity of the enzyme. However, in this case, enantioselectivity enhancement depended on the distance of the bulky substituent from the stereocenter.

To understand in more detail the experimental results, molecular modeling studies were conducted. This model included the essential parts of the enzyme highlighted in the X-ray structure shown in Figure 3, namely the active site residues, the residues involved in the oxyanion hole, and residues contributing to the hydrophobic binding pocket. All reactions discussed in the following were modeled as intermediates, which are structurally similar to the transition state. All data obtained are available in Supplementary data, but here we will showcase the most relevant cases.

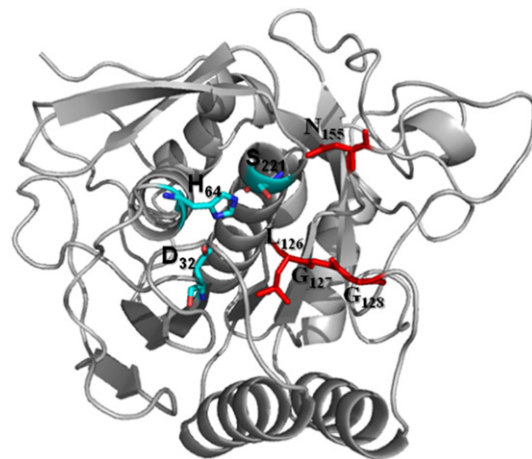


Figure 3. Scheme of the structure of subtilisin Carlsberg created using the Protein Data Bank file 1BFU. The active site residues (catalytic triad) are shown in blue, residues contributing to the hydrophobic binding pocket in red.

Computational modeling was able to explain the dependency of the enantioselectivity on the length of the linear aliphatic chain of one of the substituents at the stereocenter (**1–5**). For the smallest substrate, 2-butanol, it was found that both, *R* and *S* enantiomer fit comfortably in the binding pocket (Fig. 4). Consequently, the discrimination of the enantiomers by the enzyme is inefficient and the enantioselectivity is very low (Table 2). Increasing the length of the aliphatic chain leads to improved discrimination of the enantiomers by the enzyme. This in particular

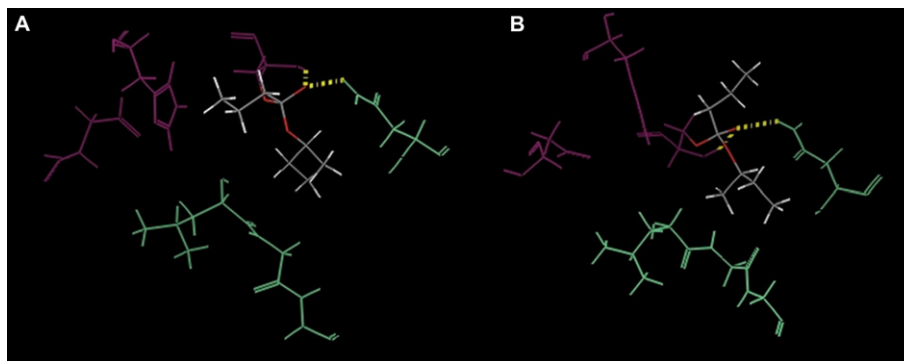


Figure 4. Results of the computational modeling of the tetrahedral intermediates of (*R*)- (A) and (*S*)-2-butanol (B). It is apparent that both substrate side chains comfortably fit into the substrate binding pocket (residues shown in green).

becomes apparent when investigating 2-heptanol and 2-octanol (Fig. 5) where the *S* enantiomer side chain comfortably fits in the binding pocket, while the *R* enantiomer simply does not.

Similar observations were made with the more bulky substrates of the second group (see Supplementary data for details). For the smallest substrate **6** the side chains of both enantiomers fit comfortably in the binding pocket. For **7** this is already not the case anymore, the *R* enantiomer side chain simply does not fit in the binding pocket anymore resulting in good discrimination of the enantiomers by the enzyme. This trend continues in **8**, but for **9** the bulky side chain of now even the *S* enantiomer does not fit well

anymore in the binding pocket and in consequence the enantioselectivity decreases.

Increasing the bulkiness of the side chain leads to even better discrimination of the enantiomers by the enzyme (third group, Table 2). For all the *S* enantiomers in this group it was found that the side chain fitted well within the binding pocket, even for **12** (Fig. 6). In contrast, for all *R* enantiomers the side chains did not fit. With increasing size of the side chain in this group and thus increasing interactions between *S* enantiomer and binding pocket, discrimination by the enzyme improved and enantioselectivity as well.

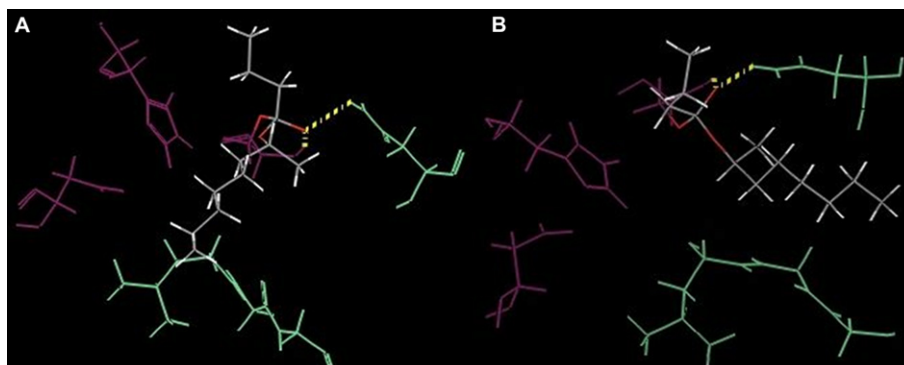


Figure 5. Results of the computational modeling of the tetrahedral intermediates of (*R*)- (A) and (*S*)-2-octanol (B). It is apparent that only the *S* enantiomer side chain comfortably fits into the substrate binding pocket (residues shown in green). The *R* enantiomer side chain does not fit into the binding pocket.

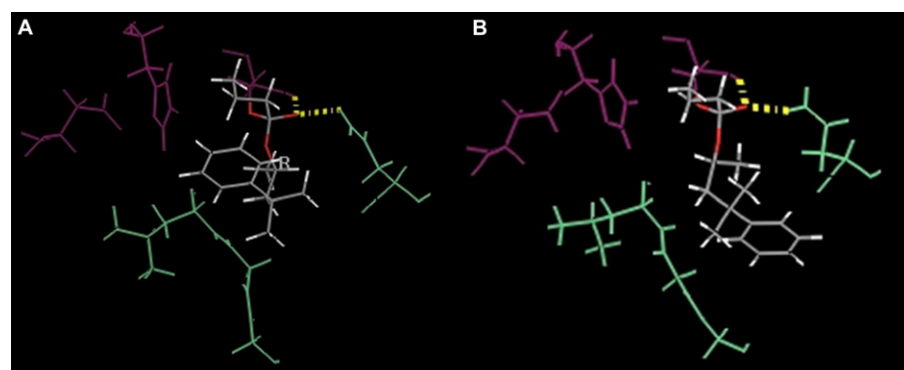


Figure 6. Results of the computational modeling of the tetrahedral intermediates of (*R*)- (A) and (*S*)-4-methyl-4-phenyl-2-pentanol (B). It is apparent that only the *S* enantiomer side chain comfortably fits into the substrate binding pocket (residues shown in green). The *R* enantiomer side chain does not fit into the binding pocket and in particular the aromatic ring has no interactions with the binding pocket.

3. Conclusions

In this study we employed an enhanced SC formulation to map the active site with respect to enantioselectivity. The empirical approach employed in this study, using a series of 14 substrates with different structures was very useful in this context and the active site of SC was systematically mapped for the first time. It was demonstrated that the substrate structure is an important factor that contributes to the enzyme enantioselectivity. Increasing the size of substrates (in particular increasing the length of a linear aliphatic chain or adding bulky groups with an optimum distance from the stereocenter) caused SC to better discriminate between the enantiomers. Computational modeling studies were conducted to analyze in detail the structural basis for the experimental results. These studies highlight that the improved discrimination of *R* and *S* enantiomer is in fact based on the length and bulkiness of the side chain. Furthermore, the experimental and computational results agree with empirical rules developed.^{13d,e} The 14 alcohols here reported should serve as a guide for predicting the enantioselectivity of SC toward similar substrates.

4. Experimental

4.1. Materials

Subtilisin Carlsberg (SC), M β CD, 2-butanol (**1**), 2-pentanol (**2**), 2-hexanol (**3**), 2-heptanol (**4**), 2-octanol (**5**), 3-methyl-2-butanol (**6**), 4-methyl-2-pentanol (**7**), 5-methyl-2-hexanol (**8**), 6-methyl-2-heptanol (**9**), 4-phenyl-2-butanol (**10**), 4,4-dimethyl-2-pentanol (**11**), 4-methyl-4-phenyl-2-pentanol (**12**), 1-phenyl-1-propanol (**13**), and 1-*p*-tolyl-1-propanol (**14**) were from Sigma-Aldrich (St. Louis, MO). Anhydrous THF was purchased from Aldrich (water content below 0.005%). Prior to use it was stored over activated molecular sieves (3 Å). Vinyl butyrate was from TCI America (Portland, OR).

4.2. Enzyme preparation

SC powder was obtained by lyophilization of a 5 mg/ml subtilisin solution in 20 mM phosphate buffer at pH 7.8 for 24 h.^{11a-c} SC co-lyophilized with M β CD was prepared in the same manner except that cyclodextrin was co-dissolved with the enzyme at a 6:1 g/g ratio of M β CD-to-enzyme prior to lyophilization.

4.3. Kinetic measurements

Product formation was followed by gas chromatography (GC). The GC instruments (Varian 3350, HP 6850, and HP 6890, with Chirasil CB columns, FID detectors, He carrier gas) were calibrated with the chiral ester products. The enzyme powder (5 mg for the lyophilized and 1 mg for the co-lyophilized preparations) was placed in a 2-mL screw-cap scintillation vial fitted with a mini-inert cap and placed in a vacuum desiccator for 4 h. The organic solvent (1.0 mL) and the substrates (140 mM of the alcohol substrate and 200 mM vinyl butyrate) were then added under nitrogen to initiate the reaction. The vial was sealed and subjected to careful sonication using a sonication bath for 10 s to homogenize the suspension. The mixture was then placed in a controlled temperature shaker and agitated vigorously at 300 rpm and 45 °C. Periodically, 0.5 μ L of the reacting solution was withdrawn and analyzed by chiral-GC. Enzyme enantioselectivity was determined by measuring the initial rates from plots of the product concentration versus time for both enantiomers. The enzyme enantioselectivity for either substrate is equal to the ratio $[k_{cat}/K_M]_S/[k_{cat}/K_M]_R = V_S[R]/V_R[S]$.^{11a} The retention times of the '*R*' and '*S*' products were obtained by using samples of the

pure enantiomers (usually the '*R*') synthesized from the corresponding alcohol enantiomers.

4.4. Synthesis of the ester products

Ester products were used to calibrate the GC instruments and were prepared as previously described with some modifications.^{16b} To a solution of (*R,S*)-alcohol (0.01835 mol) in pyridine (5 mL), butyric anhydride (8.65 mL) was added and the mixture kept at room temperature for 16 h. The mixture was poured in ice cold water and extracted with methyl tertiary butyl ether (MTBE, 3 \times 20 mL). The MTBE extract was washed with water (2 \times 10 mL), 1 N HCl (2 \times 10 mL), and finally with water (3 \times 10 mL), dried over Na₂SO₄, filtered, and the solvent was removed on a water bath maintained at 75–80 °C. The product was purified by column chromatography (silica gel 200–400 mesh, usually using 5:1 hexane/ethyl acetate). After the solvent was removed, the ester products were characterized by NMR.

4.4.1. (*R,S*)-2-Pentyl butyrate (**2b**). ¹H NMR (CDCl₃/TMS, 400 MHz), δ 0.93–1.05 (m, 6H), 1.24 (d, *J*=6.4 Hz, 3H), 1.28–1.52 (m, 4H), 1.61–1.77 (m, 2H), 2.29 (t, 2H), 4.96 (m, 1H).

4.4.2. (*R,S*)-4-Methyl-2-pentyl butyrate (**7b**). ¹H NMR (CDCl₃/TMS, 400 MHz), δ 0.88–1.06 (m, 6H), 1.25 (d, *J*=5.20 Hz, 2H), 1.28–1.37 (m, 3H), 1.61 (s, 3H), 1.64–1.78 (m, 2H), 1.90 (m, 1H), 2.30 (t, 1H), 2.49 (t, 1H), 3.79 (t, 1H).

4.4.3. (*R,S*)-5-Methyl-2-hexyl butyrate (**8b**). ¹H NMR (CDCl₃/TMS, 400 MHz), δ 0.92 (dd, *J*=6.8 Hz, 6H), 0.99 (t, 3H), 1.18–1.30 (m, 2H), 1.24 (d, *J*=6.0 Hz, 3H), 1.48–1.65 (m, 3H), 1.67 (q, 2H), 2.30 (t, 2H), 4.91–4.95 (m, 1H).

4.4.4. (*R,S*)-6-Methyl-2-heptyl butyrate (**9b**). ¹H NMR (CDCl₃/TMS, 400 MHz), δ 0.88 (d, *J*=6.4 Hz, 6H), 0.96 (t, 3H), 1.15–1.22 (m, 2H), 1.2 (d, *J*=6.4 Hz, 3H), 1.26–1.36 (m, 2H), 1.42–1.59 (m, 3H), 1.66 (q, 2H), 2.26 (t, 2H), 4.92 (m, 1H).

4.4.5. (*R,S*)-4-Phenyl-2-butyl butyrate (**10b**). ¹H NMR (CDCl₃/TMS, 400 MHz), δ 1.03 (t, 3H), 1.31 (d, *J*=6.0 Hz, 3H), 1.69–1.78 (m, 2H), 1.83–1.91 (m, 1H), 1.96–2.03 (m, 1H), 2.33 (t, 2H), 2.64–2.77 (m, 2H), 5.00–5.05 (m, 1H), 7.22–7.26 (m, 3H), 7.3–7.36 (m, 2H).

4.4.6. (*R,S*)-4-Methyl-4-phenyl-2-pentyl butyrate (**12b**). ¹H NMR (CDCl₃/TMS, 400 MHz), δ 0.92 (t, 3H), 1.11 (d, *J*=6.0 Hz, 3H), 1.39 (s, 3H), 1.40 (s, 3H), 1.49–1.56 (m, 2H), 1.73–2.03 (m, 4H), 4.95–4.99 (m, 1H), 7.19–7.23 (m, 1H), 7.32–7.38 (m, 4H).

4.4.7. (*R,S*)-1-Phenyl-1-propyl butyrate (**13b**). ¹H NMR (CDCl₃/TMS, 400 MHz), δ 0.93–1.01 (m, 6H), 1.68–1.77 (m, 2H), 1.84–2.02 (m, 2H), 2.38 (td, 2H), 5.75 (t, 1H), 7.31–7.39 (m, 5H).

4.5. Computational methods

The computer modeling results were obtained using the program MacroModel (Schrödinger Inc.) and the interface Maestro,¹⁷ frequently employed to model transition states of enzymes.¹⁸ All calculations were conducted using the OPLS-AA force field. All calculations were performed using the dielectric constant of THF (7.6) as constant. The enzyme crystal structure used was PDB entry 1BFU.¹⁹ Transition states were modeled as the tetrahedral intermediate because of their structural similarity. The initial models of the tetrahedral intermediates were sketched in the Maestro program with the carbonyl oxygen oriented toward the oxyanion hole. The system was divided in two subsets: moving residues and frozen residues. The potential binding modes of the chiral products

were first determined by using the conformational search Monte Carlo Multiple Minimum (MCM) method with 7 moving residues (Ser₂₂₁, His₆₄, Asp₃₂, Ser₁₂₅, Asn₁₅₅, Gly₁₂₇, Leu₁₂₆). The lowest energy structures that were selected had hydrogen bonds between the negatively charged oxygen of Ser₂₂₁ and the backbone NH group of Ser₂₂₁ and with the side chain NH₂ group of Asn₁₅₅. The moving residues subset later was expanded to 10 Å away from the Ser₂₂₁, but the energy minimized structures obtained did not show significant changes.

The parameters were set according to the following: the energy window for saving structures was 50 kJ mol⁻¹; the maximum iterations for minimizing the molecules were 5000 using the Polak-Ribiere Conjugate Gradient (PRCG) method; the convergence threshold was 0.001; and the other parameters were adopted default values.

Acknowledgements

This publication was made possible by grant number SC1 GM086240 (PI K.G.) from the National Institute for General Medical Sciences (NIGMS) at the National Institutes of Health (NIH) through the Support of Competitive Research (SCORE) Program. B.C. was recipient of an NIH-RISE Program doctoral fellowship (2R25 GM061151, PI Morales). Its contents are solely the responsibility of the authors and do not necessarily represent the official views of NIGMS.

Supplementary data

Supplementary data associated with this article can be found in the online version, at [doi:10.1016/j.tet.2010.01.053](https://doi.org/10.1016/j.tet.2010.01.053).

References and notes

- (a) Gotor, V. *Org. Process Res. Dev.* **2002**, *6*, 420–426; (b) Schoemaker, H. E.; Mink, D.; Wubboldts, M. G. *Science* **2003**, *299*, 1694–1697; (c) Zhu, D.; Mukherjee, C.; Hua, L. *Tetrahedron: Asymmetry* **2005**, *16*, 3275–3278; (d) Klibanov, A. M. *Nature* **2001**, *409*, 241–246; Stinson, S. C. *Chem. Eng. News* **1995**, *10*, 44; (e) Jaeger, K. E.; Eggert, T. *Curr. Opin. Biotechnol.* **2002**, *13*, 390–397.
- (a) Ghanem, A. *Tetrahedron* **2007**, *63*, 1721–1754; (b) Mahmoudian, M. *Biocatal. Biotrans.* **2000**, *18*, 105–116; (c) Koeller, K. M.; Wong, C.-H. *Nature* **2001**, *409*, 232–240; (d) Gómez-Poyou, M. T.; Gómez-Poyou, A. *Crit. Rev. Biochem. Mol. Biol.* **1998**, *33*, 53–89; (e) Carrea, G.; Riva, S. *Angew. Chem., Int. Ed.* **2000**, *39*, 2226–2254; Bordusa, F. *Chem. Rev.* **2002**, *102*, 4817–4867; Dordick, J. S. *Biotechnol. Prog.* **1992**, *8*, 259–267; Schoffers, E.; Golebiowski, A.; Johnson, C. R. *Tetrahedron* **1996**, *52*, 3769–3826.
- (a) Buckland, B. C.; Robinson, D. K.; Chartrain, M. *Metab. Eng.* **2000**, *2*, 42–48; (b) Zaks, A. *Curr. Opin. Chem. Biol.* **2001**, *5*, 130–136; (c) Patel, R. N.; Banerjee, A.; Nanduri, V.; Goswami, A.; Comezoglu, J. *Am. Oil Chem. Soc.* **2000**, *77*, 1015–1019; (d) Zaks, A.; Dodds, D. R. *Drug Discov. Today* **1997**, *2*, 513–531; (e) Jaeger, K.-E.; Reetz, M. T. *Trends Biotechnol.* **1998**, *16*, 396–403; (f) García-Urdiales, E.; Alfonso, I.; Gotor, V. *Chem. Rev.* **2005**, *105*, 313–354.
- (a) Francalanci, F.; Cesti, P.; Cabri, W.; Bianchi, D.; Martinegro, T.; Foa, M. *J. Org. Chem.* **1987**, *52*, 5079–5082.
- Wang, Y. F.; Shen, S. T.; Liu, K. K. C.; Wong, C. H. *Tetrahedron Lett.* **1989**, *30*, 1917–1920.
- Murata, M.; Terao, Y.; Achiwa, K.; Nishio, T.; Seto, K. *Chem. Pharm. Bull.* **1989**, *37*, 2670–2673.
- (a) Delinck, D. L.; Margolin, A. L. *Tetrahedron Lett.* **1990**, *31*, 3093–3096; (b) Margolin, A. L.; Delinck, D. L.; Whalon, M. R. *J. Am. Chem. Soc.* **1990**, *112*, 2849–2854.
- Ottolina, G.; Carrera, G.; Riva, S. *J. Org. Chem.* **1990**, *5*, 2366–2369.
- (a) Klibanov, A. M. *TIBS* **1989**, *14*, 141–144; (b) Castillo, B.; Mendez, J.; Al-Azzam, W.; Barletta, G.; Griebenow, K. *Biotechnol. Bioeng.* **2006**, *94*, 565–574; (c) Castillo, B.; Solá, R.; Ferrer, A.; Barletta, G.; Griebenow, K. *Biotechnol. Bioeng.* **2008**, *99*, 9–17; (d) Schmitke, J. L.; Wescott, C. R.; Klibanov, A. M. *J. Am. Chem. Soc.* **1996**, *118*, 3360–3365; (e) Secundo, F.; Carrea, G.; Soregaroli, C.; Varinelli, D.; Morrone, R. *Biotechnol. Bioeng.* **2001**, *73*, 157–163; (f) Klibanov, A. M. *TIBS* **1997**, *15*, 97–101; (g) Dordick, J. S. *Enzyme Microb. Technol.* **1989**, *11*, 194–211; (h) Luetz, S.; Giver, L.; Lalonde, J. *Biotechnol. Bioeng.* **2008**, *101*, 647–653.
- (a) Prestrelski, S. J.; Tedeschi, N.; Arakawa, T.; Carpenter, J. F. *Biophys. J.* **1993**, *65*, 661–671; (b) Griebenow, K.; Klibanov, A. M. *Proc. Natl. Acad. Sci. U.S.A.* **1995**, *92*, 10969–10976; (c) Griebenow, K.; Klibanov, A. M. *Biotechnol. Bioeng.* **1997**, *53*, 351–362.
- (a) Griebenow, K.; Díaz, Y.; Santos, A. M.; Montañez, I.; Rodríguez, L.; Vidal, M.; Barletta, G. *J. Am. Chem. Soc.* **1999**, *121*, 8157–8163; (b) Griebenow, K.; Vidal, M.; Baéz, C.; Santos, A. M.; Barletta, G. *J. Am. Chem. Soc.* **2001**, *123*, 5380–5381; (c) Santos, A. M.; Clemente, I.; Barletta, G.; Griebenow, K. *Biotechnol. Lett.* **1999**, *21*, 1113–1118; (d) Ru, M. T.; Hirokane, S. Y.; Lo, A. S.; Dordick, J. S.; Reime, J. A.; Clark, D. S. *J. Am. Chem. Soc.* **2000**, *122*, 1565–1571; (e) Eppler, R. K.; Komor, R. S.; Huynh, J.; Dordick, J. S.; Reimer, J. A.; Clark, D. S. *Proc. Natl. Acad. Sci. U.S.A.* **2006**, *103*, 5706–5710; (f) Montañez, I.; Alvira, E.; Macías, M.; Ferrer, A.; Fonseca, M.; Rodríguez, J.; González, A.; Barletta, G. *Biotechnol. Bioeng.* **2002**, *78*, 53–59; (g) Ooe, Y.; Yamamoto, S.; Kobayashi, M.; Kise, H. *Biotechnol. Lett.* **1999**, *21*, 385–389.
- (a) Broos, J. *Biocatal. Biotrans.* **2002**, *20*, 291–295; (b) Rariy, R. V.; Klibanov, A. M. *Biocatal. Biotrans.* **2000**, *18*, 401–407; (c) Broos, J.; Visser, A. J. W. G.; Engbersen, F. J.; Verboom, W.; van Hock, A.; Reinhoudt, D. N. *J. Am. Chem. Soc.* **1995**, *117*, 12657–12663.
- (a) Fitzpatrick, P. A.; Klibanov, A. M. *J. Am. Chem. Soc.* **1991**, *113*, 3166–3171; (b) Tawaki, S.; Klibanov, A. M. *J. Am. Chem. Soc.* **1992**, *114*, 1882–1884; (c) Kazlauskas, R. J. *TIBS* **1994**, *12*, 464–472; (d) Kazlauskas, R. J.; Weissfloh, A. N. E. *J. Mol. Catal. B: Enzym.* **1997**, *3*, 65–72; (e) Mugford, P. F.; Lait, S. M.; Keay, B. A.; Kazlauskas, R. J. *ChemBioChem* **2004**, *5*, 980–987.
- Persichetti, R. A.; Lalonde, J. J.; Govardhan, C. P.; Khalaf, N. K.; Margolin, A. L. *Tetrahedron Lett.* **1996**, *37*, 6507–6510.
- (a) Montalvo, B. L.; Pacheco, Y.; Sosa, B. A.; Vélez, D.; Sánchez, G.; Griebenow, K. *Nanotechnology* **2008**, *19*, 465103 (7pp); (b) Santos, A. M.; González, M.; Pacheco, Y.; Griebenow, K. *Biotechnol. Bioeng.* **2003**, *84*, 324–331.
- (a) Noel, M.; Lozano, P.; Vaultier, M.; Iborra, J. L. *Biotechnol. Lett.* **2004**, *26*, 301–306; (b) Patel, R. N. *Enzyme Microb. Technol.* **2002**, *31*, 804–826.
- (a) Chang, G.; Guida, W. C.; Still, W. C. *J. Am. Chem. Soc.* **1998**, *111*, 4379–4386; (b) Mohamadi, F.; Richards, N. G. J.; Guida, W. C.; Liskamp, R.; Lipton, M.; Caufield, C.; Chang, G.; Hendrickson, T.; Still, W. C. *J. Comput. Chem.* **1990**, *11*, 440–467.
- (a) Jiang, S.; Liao, C.; Bindu, L.; Yin, B.; Worthy, K. W.; Fisher, R. J.; Burke, T. R., Jr.; Nicklaus, M. C.; Roller, P. P. *Bioorg. Med. Chem. Lett.* **2009**, *19*, 2693–2698; (b) Jiang, J.-K.; Ghoreschi, K.; Deflorian, F.; Chen, Z.; Perreira, M.; Pesu, M.; Smith, J.; Nguyen, D.-T.; Liu, E. H.; Leister, W.; Costanzi, S.; O'Shea, J. J.; Thomas, C. J. *J. Med. Chem.* **2008**, *51*, 8012–8018.
- Schmitke, J. L.; Stern, L. J.; Klibanov, A. M. *Biochem. Biophys. Res. Commun.* **1998**, *248*, 273–277.